

Cite this article as: Su Jinlong, Luo Cui, Ruan Ye, et al. Microstructure and Properties of Soldered Joints of Cu/Ni-Coated Sintered-NdFeB Permanent Magnets and DP1180 Steel[J]. Rare Metal Materials and Engineering, 2024, 53(02): 365-370. DOI: 10.12442/j.issn.1002-185X.20230514.

ARTICLE

Microstructure and Properties of Soldered Joints of Cu/Ni-Coated Sintered-NdFeB Permanent Magnets and DP1180 Steel

Su Jinlong^{1,2}, Luo Cui³, Ruan Ye¹, Qiu Xiaoming¹, Xing Fei^{1,2}

¹Key Laboratory of Automobile Materials Ministry of Education, Jilin University, Changchun 130022, China; ²Shenzhen Research Institute of Jilin University, Shenzhen 518057, China; ³Shanghai Aerospace Control Technology Research Institute, Shanghai 201109, China

Abstract: Zn-6Sn-5Bi alloy was used to solder DP1180 steel and NdFeB permanent magnet coated with Cu and Ni, and the microstructures and mechanical properties of the soldered joints under different coating conditions were compared and analyzed. Results show that for the soldered joint of sintered NdFeB permanent magnet with Cu coating and DP1180 steel, Cu diffuses in the solder and reacts with Zn and Fe to form brittle intermetallic compounds, resulting in cracks and holes in the soldering seam. The shear strength of the soldered joint of sintered NdFeB permanent magnet with Cu coating and DP1180 steel decreases to 52.3 MPa, compared with that without Cu coating (61.9 MPa). For the soldered joint of sintered NdFeB permanent magnet with Ni coating and DP1180 steel, Ni is concentrated at the interface of NdFeB side, different diffusion layers are formed due to the diffusion of Sn and Bi, and the shear strength of soldered joint increases to 78.1 MPa.

Key words: sintered NdFeB permanent magnet; metal coating; soldered joint; microstructure; shear strength

As a functional material with strong magnetism, sintered NdFeB permanent magnet has the characteristics of high remanence, high coercivity, and high magnetic energy product, which is widely used in the hybrid vehicles, electronic information, and medical equipment^[1-2]. The sintered NdFeB permanent magnet is usually prepared by powder metallurgy, therefore showing poor processing performance. Thus, large-size components with complex shapes can hardly be produced. The sintered NdFeB permanent magnet can exert excellent magnetic properties to meet the requirements of modern manufacture industry by connection with steel or other metal carriers^[3]. Currently, the commonly used connection methods of sintered NdFeB permanent magnet are mechanical connection and adhesive connection, which have low precision, low conductivity, and difficulty in satisfying the manufacture of small-size structures^[4-5].

The sintered NdFeB permanent magnet is extremely sensitive to the temperature change. High temperature destroys

the lattice structure of sintered NdFeB permanent magnet, and even degrades its magnetic properties. Brazing can ensure that the base metal does not melt, thereby exerting a little impact on the microstructure and properties of the base metal. Thus, the sintered NdFeB permanent magnet and steel after brazing have been widely researched. However, the effect of coating on sintered NdFeB permanent magnet during brazing is rarely reported^[6-8]. The sintered NdFeB permanent magnet is prone to electrochemical corrosion because of its multiphase structure and large interphase potential difference^[9]. Therefore, the sintered NdFeB permanent magnet is usually covered by metal coating in actual industrial applications^[10-11]. Common metal coatings involve the Zn, Al, Ni, and Cu elements, which are prepared through the electroplating and electroless plating^[12-14]. In this research, the Zn-Sn-Bi alloy was used as solder to braze steel and sintered NdFeB permanent magnet with Cu or Ni coating. The microstructures and mechanical properties of the soldered joints were studied, and the

Received date: August 21, 2023

Foundation item: Creation and Development Technology Project of Shenzhen, China (2021Szvup050); Shanghai Sailing Program (23YF1417400); 2020 Renewal Program of Jilin University (419080520464)

Corresponding author: Xing Fei, Ph. D., Key Laboratory of Automobile Materials Ministry of Education, Jilin University, Changchun 130022, P. R. China, E-mail: xingfei@jlu.edu.cn

Copyright © 2024, Northwest Institute for Nonferrous Metal Research. Published by Science Press. All rights reserved.

influence mechanism of coating on the microstructure and properties of the soldered joints was analyzed.

1 Experiment

In this experiment, the sintered NdFeB permanent magnet ($\Phi 10\text{ mm}\times 10\text{ mm}$) and DP1180 steel ($20\text{ mm}\times 20\text{ mm}\times 1.2\text{ mm}$) were used as base metal. Fig.1 shows the microstructures of sintered NdFeB permanent magnet and DP1180 steel. The sintered NdFeB permanent magnet consists of $\text{Nd}_2\text{Fe}_{14}\text{B}$ and white Nd-rich phase. The DP1180 steel is composed of massive martensite and ferrite containing carbides. Table 1 shows the chemical composition of sintered NdFeB permanent magnet and DP1180 steel. The solder used in the experiment was the Zn-6Sn-5Bi alloy with the thickness of $200\text{ }\mu\text{m}$, which was placed between NdFeB magnet and steel. During the soldering process, the vacuum condition was set as $1\times 10^{-1}\text{ Pa}$, and Ar was pumped at the rate of 0.4 L/min . The specimen was heated to $430\text{ }^\circ\text{C}$ at the heating rate of $10\text{ }^\circ\text{C/s}$ and cooled to room temperature after holding at designed temperature for 30 s . The shear properties of the soldered joints were tested at the loading rate of 0.1 mm/min .

2 Results and Discussion

Fig.2 presents the microstructures of soldered joint of Cu-coated NdFeB magnet and steel. Table 2 shows the results of element composition analysis of different points in Fig.2. The microstructure of the soldering seam becomes uneven, compared with that without coating^[8]. Cracks and pores appear in the soldering seam. According to the microstructure and element analysis results of Fig.2b, the atomic ratio of Cu:Zn is approximately 1:6 in the A_1 point. Based on the Cu-Zn phase diagram, the phase at reaction layer is $\epsilon\text{-CuZn}_6$. The Cu content of A_2 and A_3 points is significantly lower than that of A_1 point. The A_2 point is rich in Zn, Sn, and Bi elements. The microstructure and element analysis of the interface at steel side are shown in Fig.2c and Table 2, respectively. During the soldering process, Fe element in the steel is diffused into the soldering seam. As shown in Fig.2e, the Fe diffusion layer is about $20\text{ }\mu\text{m}$ in width, which corresponds to the cracks of soldering seam. According to Table 2, the A_4 , A_5 , and A_6 points are rich in Zn element. Cu is enriched at both NdFeB side and steel side. Due to the Cu coating on the NdFeB surface, NdFeB magnet has higher Cu content than the steel side does.

Fig.3 shows the microstructure and composition analysis of the soldered joint of Ni-coated NdFeB magnet and steel. Table 3 shows the element composition results of different points in Fig.3. Unlike the soldered joints of Cu-coated NdFeB magnet, there are no obvious defects in the soldered joints of Ni-coated NdFeB magnet and steel. As shown in Fig. 3b, the

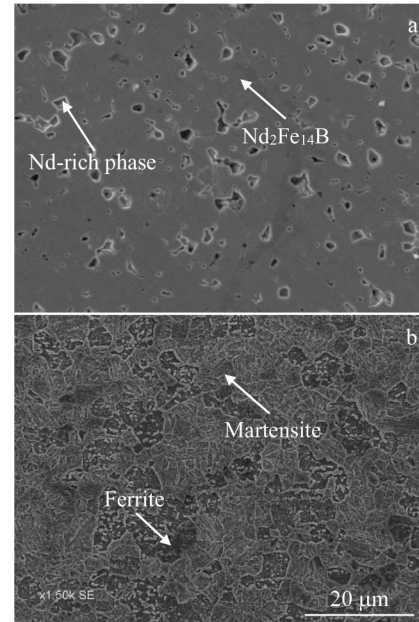


Fig.1 Microstructures of base materials: (a) sintered NdFeB permanent magnet and (b) DP1180 steel

interface microstructure on NdFeB side is composed of two layers with width of 15 and $10\text{ }\mu\text{m}$, and the main elements are Zn and Ni. Compared with those of the interface microstructure of B_1 point, the Sn and Bi contents at B_2 point of interface are higher. The Ni content of the interface microstructure at steel side is lower than that at NdFeB side. According to the chemical composition results and Fe-Zn phase diagram, the microstructures at B_4 and B_5 points are composed of $\Gamma\text{-FeZn}_{11}$. Due to the short-range diffusion of Sn atoms in the solder, the Sn content at B_4 point is higher than that at B_5 point. The diffusion layer between steel and solder (B_6 point) is $\Gamma\text{-Fe}_3\text{Zn}_{10}$, which is consistent with the results in Ref.[8]. It can be seen that Ni is mainly concentrated near the interface at NdFeB side, and it does not diffuse to the interface of soldering seam and steel side^[8].

Based on the microstructure analysis of soldered joints, Fig. 4 shows the evolution mechanism of soldered joints of coated NdFeB magnet and steel. When the temperature reaches the melting temperature of the solder, due to the concentration gradient between solder and base metal, the elements in solder diffuse to the substrate. Eq.(1) can be used to calculate the chemical affinity between different elements:

$$\eta = \left(\frac{z}{r_K} \right)_A + \Delta X \quad (1)$$

$$\left(\frac{z}{r_K} \right)_B$$

Table 1 Chemical composition of sintered NdFeB permanent magnet and DP1180 steel (at%)

Sintered NdFeB permanent magnet	Element	Nd	Fe	B	Dy	Co	Cu	Al	Zr	-	-
	Content	23.00	73.61	1.10	1.50	0.50	0.03	0.25	0.01	-	-
DP1180 steel	Element	C	Mn	Cr	Si	Mo	P	Nb	S	Ti	Fe
	Content	0.15	2.59	0.67	0.09	0.07	0.04	0.03	0.01	0.02	Bal.

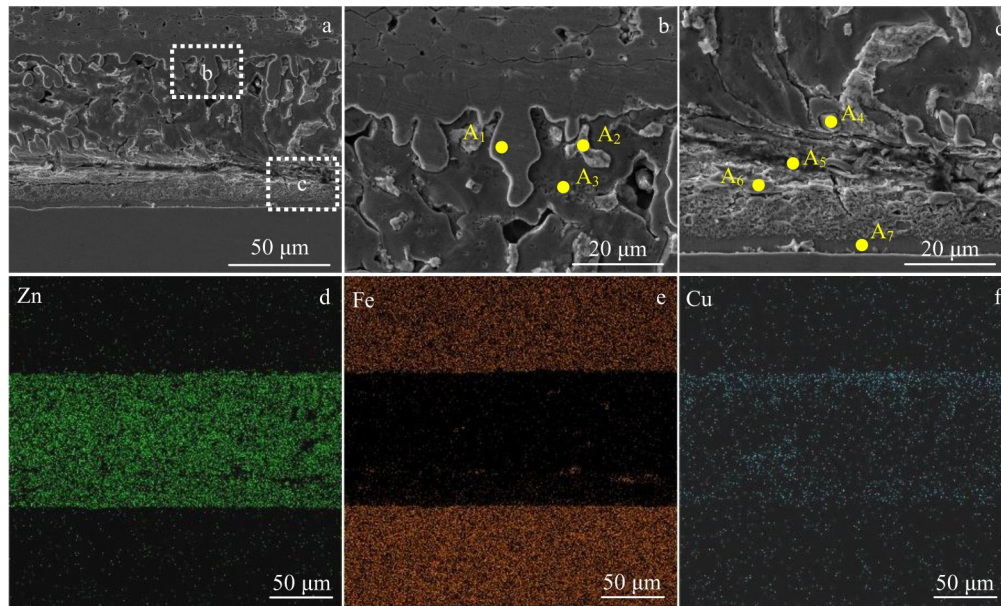


Fig.2 Microstructures (a–c) and element distributions (d–f) of soldered joints of Cu-coated NdFeB magnet with steel: (a) cross-section of joint; (b) interface at NdFeB side; (c) interface at steel side; (d) Zn element in soldered joint; (e) Fe element in soldered joint; (f) Cu element in soldered joint

Table 2 Chemical composition of different points marked in Fig.2 (at%)

Point	Fe	Cu	Zn	Sn	Bi
A ₁	0.61	13.53	85.85	-	-
A ₂	2.25	1.19	43.50	4.52	48.53
A ₃	0.41	2.09	97.50	-	-
A ₄	5.04	8.75	83.47	2.46	0.27
A ₅	3.79	2.33	88.43	4.17	1.27
A ₆	5.50	5.75	83.75	3.90	1.09
A ₇	97.51	0.16	2.29	0.03	-

where η is the chemical affinity parameter; Z/r_k is the charge/radius ratio; the subscripts A and B represent element A and B, respectively; ΔX is the electronegativity difference between element A and B. Large η value indicates the strong interactions between element A and B, and the two elements are easier to form chemical bonds. The calculated η values of Cu-Zn and Ni-Zn binary systems are 2.85 and 1.25, respectively, indicating that Cu-Zn has greater chemical affinity than Cu-Ni does. Thus, the irregular interface forms at Cu-coated NdFeB side of the soldered joint, and the long-range diffusion of Cu atoms is achieved in the soldering seam, compared with those of the soldered joint of Ni-coated NdFeB magnet and steel, as shown in Fig.4.

When the Cu atoms diffuse to the steel side, the Cu, Zn, and Fe atoms gradually combine together. According to the atomic ratio of the three elements and the Cu-Fe-Zn ternary alloy phase diagram (Fig.5)^[15], it can be seen that the L+ FeZn₁₀+ ζ mixed phase is formed in the soldering seam during the soldering process. Due to the brittleness of ζ phase, cracks and holes are generated in the soldering seam. More Fe atoms are participated in the reaction, resulting in the increased

brittleness of soldering seam and forming larger cracks in the soldering seam near the steel side. Significant chemical affinity occurs between Ni and Sn, as well as between Ni and Bi. Sn and Bi atoms in the soldering seam diffuse into the Ni coating. Due to different degrees of diffusion, the interface at NdFeB side can be divided into two parts. A large number of Ni atoms are concentrated near the NdFeB interface, and only a small number of Ni atoms diffuse into the soldering seam, which maintains the microstructure and original shape of soldering seam.

Fig.6 shows the shear properties of different soldered joints. The shear strength of soldered joint of Cu-coated NdFeB magnet and steel is 52.3 MPa, and that of the soldered joint of Ni-coated NdFeB magnet and steel is 78.1 MPa. The shear strength of the soldered joint of NdFeB magnet without coating and steel is 61.9 MPa^[8]. The soldered joint of Cu-coated NdFeB magnet and steel contains a large number of cracks, and the crack near the steel side becomes obvious during the shearing process, resulting in the decrease in mechanical properties. The shear performance of soldered joints of Ni-coated NdFeB magnet and steel is better than that

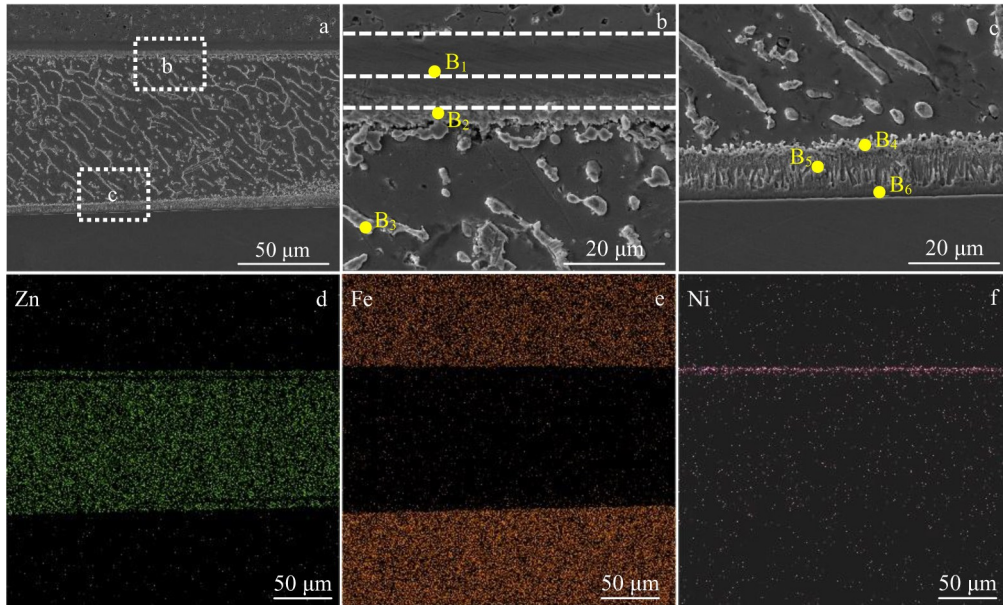


Fig.3 Microstructures (a–c) and element distributions (d–f) of soldered joints of Ni-coated NdFeB magnet with steel: (a) cross-section of joint; (b) interface at NdFeB side; (c) interface at steel side; (d) Zn element in soldered joint; (e) Fe element in soldered joint; (f) Ni element in soldered joint

Table 3 Chemical composition of different points marked in Fig.3 (at%)

Point	Fe	Ni	Zn	Sn	Bi
B ₁	0.37	14.72	82.40	2.39	-
B ₂	0.60	11.44	78.64	8.48	0.66
B ₃	1.26	2.05	95.84	0.52	0.33
B ₄	8.44	0.18	87.86	2.97	-
B ₅	8.64	0.43	89.41	1.30	0.22
B ₆	28.66	0.06	70.87	0.35	0.06

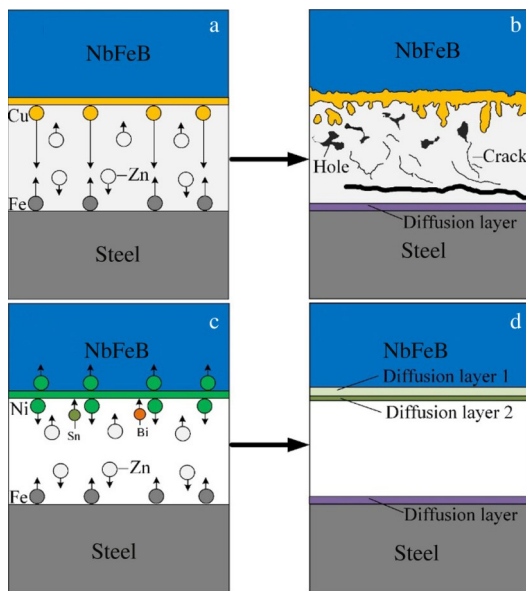


Fig.4 Schematic diagrams of interface microstructure evolution and element diffusion in soldered joints of Cu-coated (a–b) and Ni-coated (c–d) NdFeB magnet with steel: (a, c) element diffusion in soldered joints; (b, d) characteristics of soldered joints

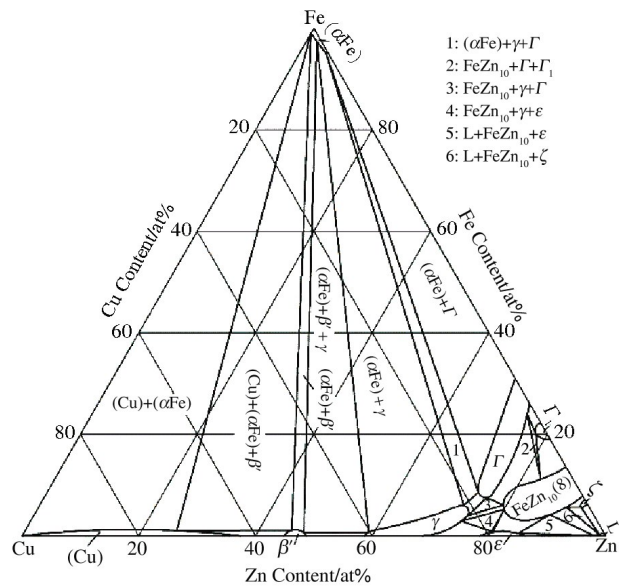


Fig.5 Phase diagram of Cu-Fe-Zn ternary alloy^[15]

of the soldered joints of uncoated NdFeB magnet and steel. The fracture is located between the diffusion layer 2 at NdFeB

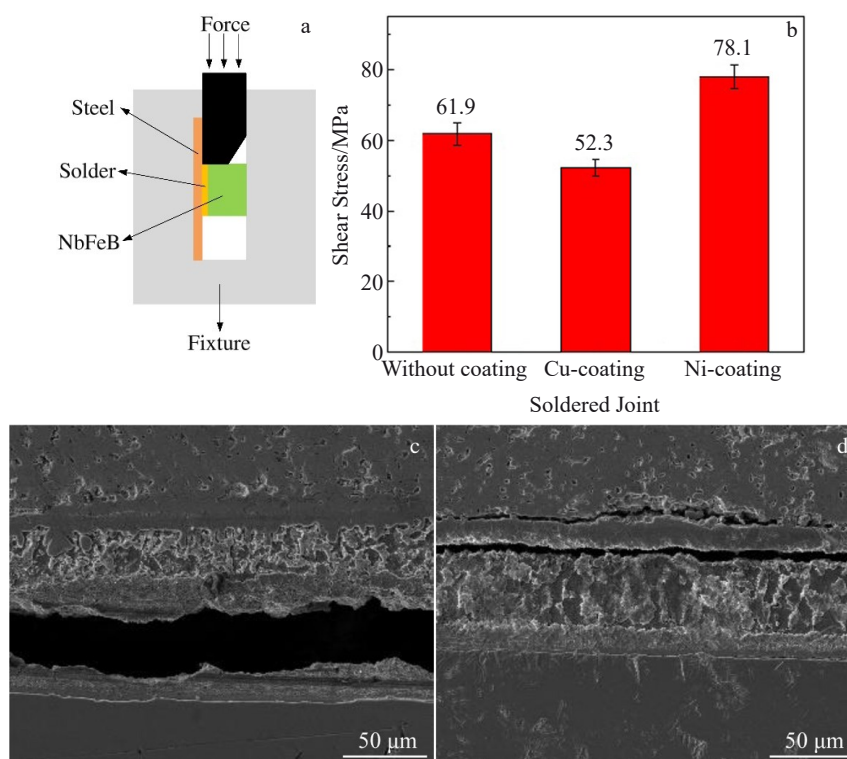


Fig.6 Schematic diagram of shear test (a); shear properties of different soldered joints (b); fracture morphologies of soldered joints of Cu-coated (c) and Ni-coated (d) NdFeB magnet with steel

side and the soldering seam, indicating that the diffusion of Ni atoms in the soldering seam can enhance the mechanical properties of the soldering seam. The diffusion layer 2 formed by Sn element diffusion has a weak bonding performance with the soldering seam.

3 Conclusions

1) For the soldered joints of Cu-coated NdFeB magnet and DP1180 steel, Cu/Zn of the solder and Fe of the base metal react to form brittle intermetallic compounds, resulting in cracks and pores in the soldering seam. Thus, the shear strength decreases.

2) For the soldered joints of Ni-coated NdFeB magnet and DP1180 steel, Ni is mainly concentrated on the interface at NdFeB side. The interface can be divided into two diffusion layers due to different contents of Sn and Bi elements. The shear strength of the soldered joint is enhanced.

References

- Li J, Bian Y, Xu K et al. *Materials Letters*[J], 2020, 267: 127537
- Kim T H, Sasaki T T, Ohkubo T et al. *Acta Materialia*[J], 2019, 172: 139
- Chang B H, Bai S J, Du D et al. *Journal of Materials Processing Technology*[J], 2010, 210(6-7): 885
- Je S S, Rivas F, Diaz R E et al. *IEEE Transactions on Biomedical Circuits and Systems*[J], 2009, 3: 348
- Kim H J, Kim D H, Koh C S et al. *IEEE Transactions on Magnetics*[J], 2009, 43(6): 2522
- Luo C, Qiu X M, Su J L et al. *Journal of Manufacturing Processes*[J], 2021, 67: 487
- Luo C, Qiu X M, Su J L et al. *Journal of Manufacturing Processes*[J], 2021, 64: 323
- Luo C, Qiu X M, Ruan Y et al. *Materials Science and Engineering A*[J], 2020, 792: 139832
- Chen W, Huang Y L, Luo, J M et al. *Journal of Magnetism & Magnetic Materials*[J], 2019, 476: 134
- Fernengel W, Rodewald W, Blank R et al. *Journal of Magnetism and Magnetic Materials*[J], 1999, 196: 288
- Zhang P J, Liu Q, Sun W et al. *Rare Metal Materials and Engineering*[J], 2022, 51(8): 2863
- Shen L D, Wang Y H, Jiang W et al. *Corrosion Engineering Science and Technology*[J], 2017, 52(4): 311
- Ding J J, Xu B J, Ling G P et al. *Applied Surface Science*[J], 2014, 305(1): 309
- Chen R J, Wang Z X, Xu T et al. *Chinese Physics B*[J], 2018, 27(11): 75
- Raghavan V. *Journal of Phase Equilibria and Diffusion*[J], 2013, 34(3): 230

镀铜/镍烧结钕铁硼永磁体与DP1180钢钎焊接头的组织与性能

苏金龙^{1,2}, 罗萃³, 阮野¹, 邱小明¹, 邢飞^{1,2}

(1. 吉林大学 汽车材料教育部重点实验室, 吉林 长春 130022)

(2. 吉林大学 深圳研究院, 广东 深圳 518057)

(3. 上海航天控制技术研究所, 上海 201109)

摘要: 采用 Zn-6Sn-5Bi 钎料对镀 Cu/Ni 的烧结 NdFeB 永磁体和 DP1180 钢进行钎焊连接, 对比分析了 2 种镀层条件下钎焊接头的微观组织和力学性能。结果表明, 对于镀 Cu 的烧结 NdFeB 永磁体和 DP1180 钢的钎焊接头, Cu 在钎料中扩散并与 Zn、Fe 反应生成脆性金属间化合物, 导致钎缝中出现裂纹和孔洞。与无镀层时的烧结 NdFeB 永磁体和 DP1180 钢的钎焊接头相比, 接头的剪切强度由 61.9 MPa 降低至 52.3 MPa; 对于镀 Ni 的烧结 NdFeB 永磁体和 DP1180 钢的钎焊接头, Ni 集中分布在 NdFeB 一侧的界面处, 并且由于 Sn 和 Bi 的扩散形成了不同的扩散层, 其剪切强度提高至 78.1 MPa。

关键词: 烧结 NdFeB 永磁体; 金属镀层; 钎焊接头; 微观组织; 剪切强度

作者简介: 苏金龙, 男, 1993 年生, 硕士, 工程师, 吉林大学汽车材料教育部重点实验室, 吉林 长春 130022, E-mail: sujinkl@jlu.edu.cn